Keywords: Sustainable Fuels, Alternative Fuels, Future Fuels, Shipping Decarbonisation, Methanol, Marine engine retrofit technologies

Methanol retrofit technologies, from concept to engine operation: Performance and emissions evaluations on a large bore engine

Dr. Ludovico Viglione[1], Dr. Marios Ioannou[1], Alejandro Calvo Oliveira[1], Gennaro Caputo[2], Dr. Thorsen Sven Lauge[3], Placanica Michele[2]

[1]Wärtsilä Services Switzerland AG, [2]Wärtsilä Italia S.p.A., [3]Wärtsilä Danmark A/S

https://doi.org/10.18453/rosdok_id00004646

Abstract

IMO's Greenhouse Gas reduction strategy is one of the biggest challenges that the shipping industry faces. While intermediate measures of reducing emissions from ships are currently available, the reduction targets set by IMO for 2050 can only be met through the use of sustainable fuels that will gradually replace diesel. Methanol has been identified as one of the low carbon fuels that could decarbonise shipping, and results from recent investigations confirmed its strong potential in reducing GHG emissions if utilized as a marine fuel. This paper describes the approach that was adapted by Wärtsilä to retrofit a 2-stroke marine diesel research engine with existing systems and components to operate on Methanol. The workflow comprised of the development of a 3-D CFD model of the Wärtsilä 6RT-Flex50-B (RTX-5), which was calibrated with experimental data obtained from the combustion of methanol in a spray chamber. The outcomes from the numerical analysis were applied to define the nozzle tip configurations for the methanol injectors, and following an optimisation study, the best configurations were identified, designed and manufactured for use on the real engine. The conversion of the engine with the required hardware, and the development of the combustion system through numerical analysis, were executed in parallel. The main characteristics of the retrofit system are summarized, with focus on the key upgrades that were made to a high-pressure pump, a common rail system and fuel injectors, to achieve operation of the 6-cylinder 2-stroke marine engine on methanol. The study concludes with the results from the engine performance and emission measurements that were conducted on the engine, which was fully instrumented for the testing purposes. The analysis demonstrated that when the dual-fuel engine was operated on Methanol, it was considerably more efficient than when operated on conventional Diesel, with also significant reductions of NO_x emissions due to lower combustion temperatures, and of CO_2 emissions through reductions in fuel consumption.

1. Introduction

Methanol has been widely investigated as a potential fuel since the early stages of internal combustion engines. Its chemical and physical properties, industrial availability, and low carbon to hydrogen ratio, make this low-carbon alcohol attractive as an alternative to traditional fossil fuels. The use of light alcohols, such as methanol or ethanol, in spark-ignition engines seems relatively straightforward, and has been extensively analysed in the literature [1]. Methanol's high octane number and latent heat of evaporation, as well as its low air to fuel ratio (Table 1) enable this fuel to be particularly suitable in such applications, both as a standalone fuel, or as a blend with gasoline. On the contrary, the long ignition delay and the subcooling effect of methanol pose some challenges for its application in compression-ignition engines. Some examples of methanol direct injection as single fuel in heavy duty engines can be found in the literature where fuel autoignition is achieved by means of fuel additives [2] and increased compression ratios of up to 1:28 [3,4].

A more common approach is the adaptation of a dual fuel system, where methanol ignition is achieved through the use of a pilot fuel of higher reactivity, typically diesel. Two main strategies can be identified in the literature with regards to dual fuel operation: methanol port fuel injection, also referred as methanol "fumigation", or direct dual fuel injection, where both fuels are injected inside the cylinder (combustion chamber).

Focusing on the in-cylinder injection strategies, these can be distinguished as premixed combustion and diffusive combustion. The premixed combustion of methanol in a direct injection (DI) system was directly compared to a port-fuel injection (PFI) system [5], and the results did not reveal any significant benefits in the DI system. Instead, it was observed that for the DI system spray targeting, in relation to fuel mixing and wall wetting, had a strong impact in the emissions of HC, CO and Soot.

Direct injection with diffusive methanol combustion has been more recently applied to four-stroke engines and resulted in better combustion stability when compared to both, PFI and DI premixed strategies [6,7]. During this strategy, methanol is injected late in the compression stroke, near top dead center. Studies showed that increasing the level of methanol share led to reduced combustion duration with benefits on thermal efficiency, and therefore fuel consumption. Further application of the diffusive combustion system on marine engines [8] confirmed the combustion stability of the system and the strong importance of good spray targeting to maximize the interaction between the pilot and the main fuel across several engine loads.

The current paper discusses the methodology to design and develop a dual fuel retrofit concept of diffusive combustion on existing large bore 2-stroke low-speed marine engines. The study addresses the impact of different injector nozzle tip designs, which affect the spray pattern of methanol, the effect of different injection strategies and the overall engine tuning strategy by means of a numerical and experimental analysis.

Experimental activities were first carried out in a spray chamber that was optically accessible, and subsequently on a two-stroke 6-cylinder marine test engine (RTX5).

Table 1: Fuels properties [9]

	Methanol (CH_3OH)	Ethanol (C_2H_5OH)	LFO
Density [kg/m3]	792	785	835
Heat of Vaporization [MJ/kg]	1.168	0.919	0.270
Lower Heating Value [MJ/kg]	19.99	26.9	43.2
RON	109	109	n.d.
Stoichiometric A/F Ratio [kg/kg]	6.46	8.98	14.95

2. Methodology and tools

To define the computational methods the authors aimed for a good compromise between model accuracy and computational time, in consideration of the large engine size and the need of a robust tool to drive the design phase of a commercial retrofit kit. The computational models described in the next section were developed in OpenFoam environment with the additional use of a customized library "LibICE" developed by Politecnico di Milano [10]. The numerical model is based on RANS approach, the turbulence closure is addressed with the k-ϵ model, while the injection of both fuels is represented with a Lagrangian method and Reitz-Diwakar breakup model. The combustion is modelled with a perfectly stirred reactor model that accounts for both fuels. Two approaches were evaluated to solve the chemical reactions, the direct chemistry solution and a tabulated approach. The latter resulted to be equally accurate and faster than the former, and was therefore selected for the full engine model.

2.1. Optical combustion chamber and CFD model description

The combustion concept assessment and the initial validation of the numerical framework was performed in an optically accessible combustion chamber, where different spray orientations and injection strategies were tested, and subsequently utilized for the validation of the numerical models. The experimental chamber [11] developed by Wärtsilä Services Switzerland in collaboration with CNR STEMS, was specifically designed to replicate the geometry and the thermodynamic condition of a large bore marine engine (Figure 1). Two injectors, one acting as a pilot and the other as main injector, were fitted on the top end of the chamber, opposite to a sapphire window. To reproduce as close as possible the spray characteristics of the target engine, both the injectors were sized for 2-stroke marine applications, filling a gap in the available literature often oriented towards automotive size injectors. The injectors were located in eccentric position, at the same radial distance, in specially designed pockets that provided the option to freely rotate them along their respective axes, and therefore allow for the investigation of various spray interactions between the two fuels.

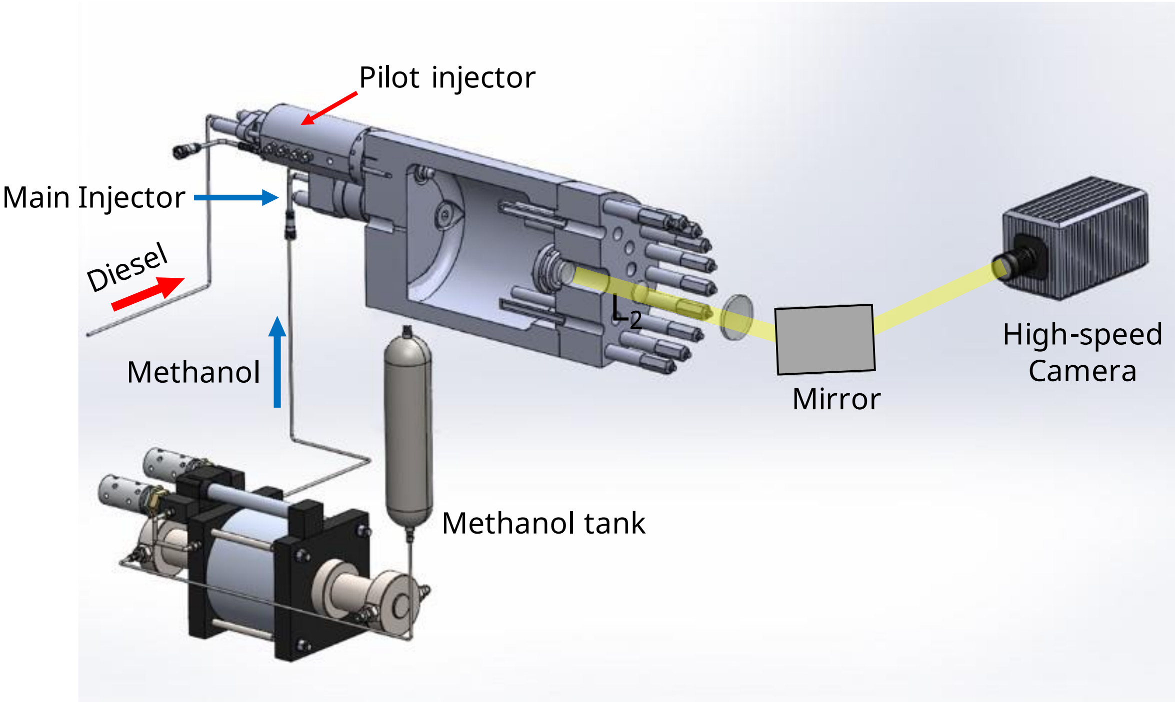

Figure 1: Optical accessible combustion chamber

Figure 2 depicts the meshes used to discretize the optical combustion chamber, where a hexahedral non-structured grid was applied with static local refinements in the combustion zone. A summary of the mesh characteristics with the respective computational times are reported in Table 2. The mesh independence check performed on the grids (Figure 3) demonstrated a small pressure sensitivity on the selected grid, and for this reason a medium grid was chosen for the tests to save computational time and maintain consistency with the grid structure utilized in the full engine tests.

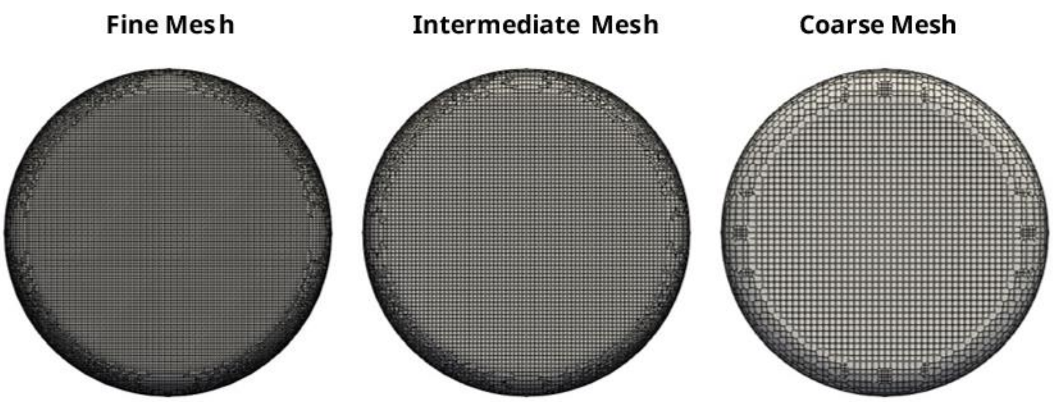

Figure 2: Mesh independence test - Hexaedral mesh for optical combustion chamber

Table 2: Mesh independence test - base cell sizes and computational time

Mesh size and computational time			
	Cell Count (x 10³)	**base mesh [mm]**	**simulation time [h]**
Coarse	~ 109	6	~3
Medium	~ 323	4	~9
Refined	~ 745	3	~20

A well stirred reactor model was selected for the combustion simulation [12] and with this approach each cell is treated as a homogeneous reactor accounting for the dual fuel combustion. The chemical reaction rates were separately tabulated with two different chemical mechanisms, namely the NUIGMech1.0 [13] for n-heptane (used as diesel surrogate) and the CRECK DME model [14] for Methanol. The chemical decoupling of the two fuels was justified by the fact that the low quantity of the injected diesel was considered to not interact chemically with the main fuel. To assess the effectiveness of the double tabulation method, it was found necessary to compare it with the established direct chemistry integration method. While the reacting flow simulation with the direct chemical implementation method was time consuming (due to the extra computational overhead), a good computational improvement was implemented through use of the Dynamic Load Balancing method – DLBFoam [15].

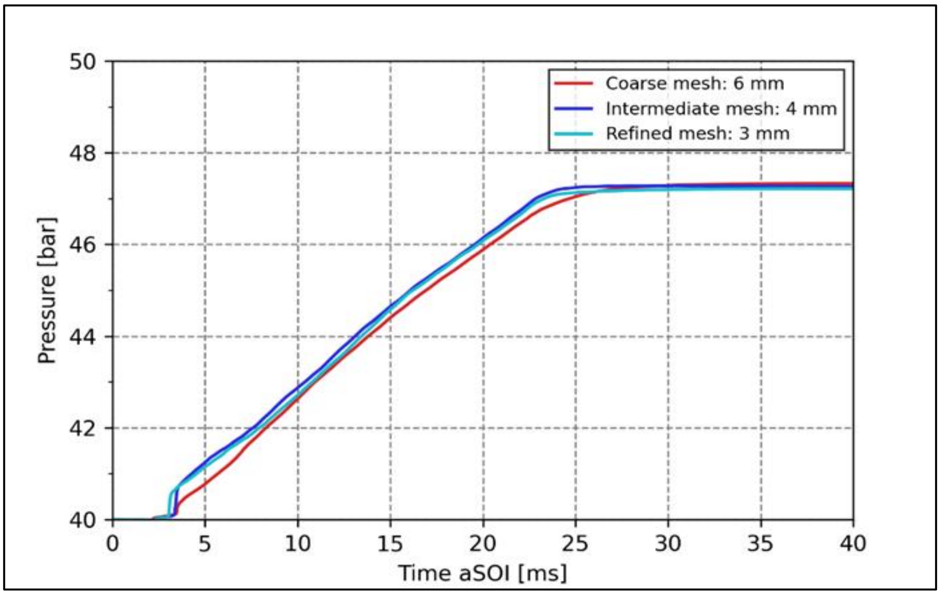

Figure 3: Optical combustion chamber mesh independence - CFD model pressure sensitivity

The comparison of the results between the two methods in Figure 4 show the satisfactory alignment between the tabulated and the direct kinetic approaches, where the pressure curves from both cases were very similar. The small differences identified at the early stages of combustion and in the evolution of the temperature contour had no significant impact on the overall measured quantity, therefore confirming the similarity of both methodologies.

The selected "intermediate mesh" and the tabulated chemistry approach were compared with the experimental data (Figures 4 and 5), and the pressure trace correlation was considered sufficient enough to justify the adaptation of these methodologies for the simulation of the full engine.

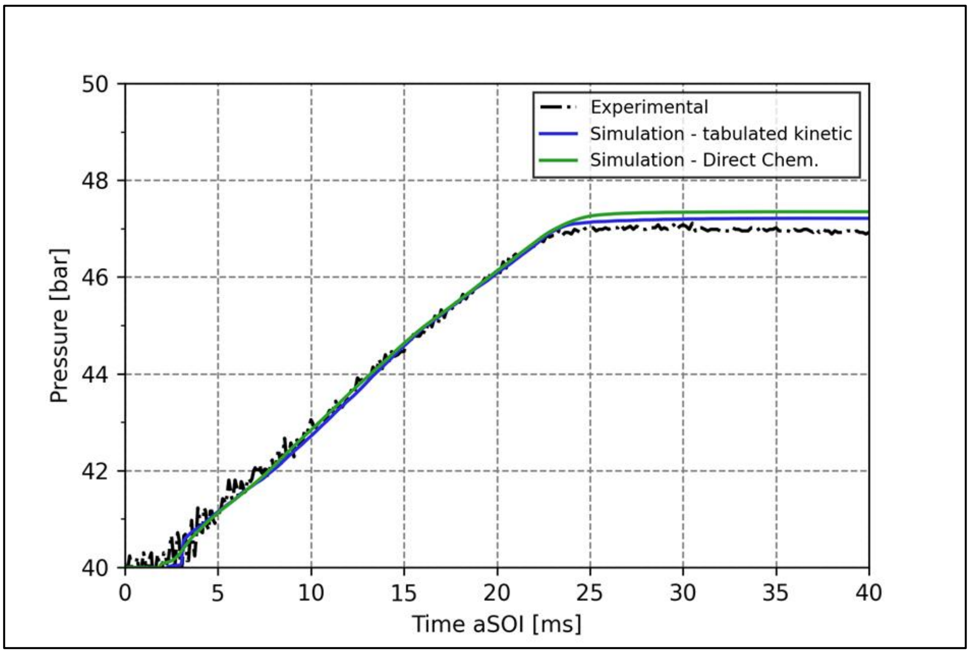

Figure 4: Combustion model validation - Experimental pressure measurement vs. Simulation results with tabulated kinetic and direct chemical integration model

2.2. Engine model

The numerical setup described for the optical combustion chamber was also applied to the R&D laboratory engine (RTX5), which is a Wärtsilä 6RT-Flex50-B 2-stroke uniflow scavenging marine engine, of 500 mm bore, 2050 mm stroke, and 6-cylinders in-line. Main engine parameters are reported in Table 3.

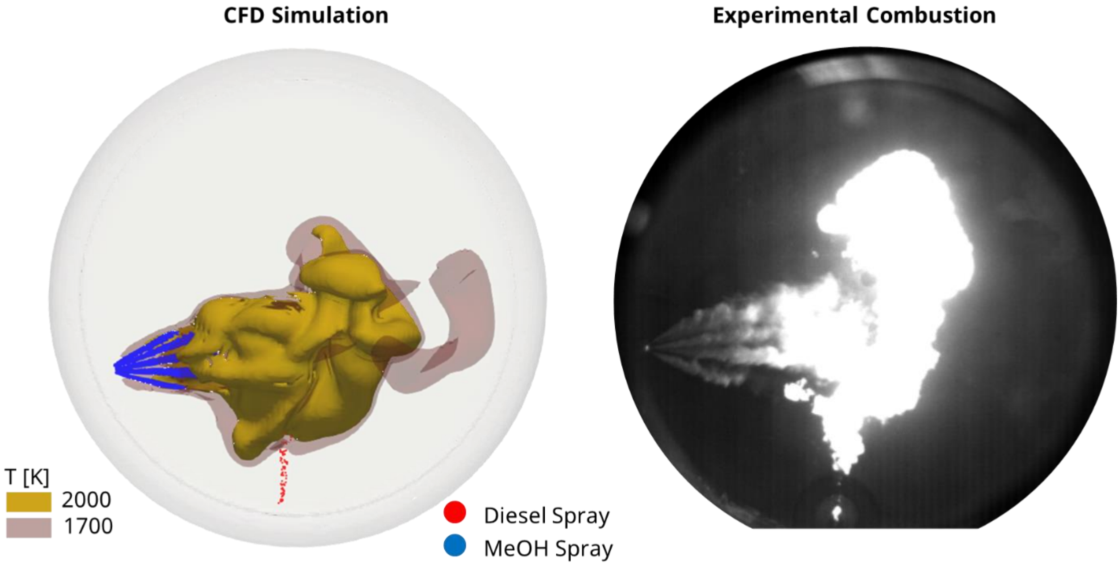

Figure 5: Optical combustion chamber test - CFD simulation results (temperatures iso-contours and lagrangian sprays) compared with experimental images of visible flame

To achieve a reasonable computational time for the complete engine simulation a base mesh size of 12 mm was applied to simulate the scavenging phase. Localized refinements were employed in the proximity of the intake ports and in the exhaust valve region to gain accuracy without compromising the total cell count. The injection and combustion phases were then computed with a more refined mesh, where the base size was set to 2.5 mm, and local conical refinement was applied in the vicinity of the nozzles during the injection process. A complete 1-D engine model was selected as the source to impose pressure and temperature values on the cylinder intake and exhaust boundaries, and a similar approach was applied to compute the injection mass flow rate for both fuels.

Table 3: Engine description

Engine Parameters	
Engine Type	Two-stroke RTX5
Number of Cylinders	6
Bore [cm]	50
Stroke [m]	2.05
Power [kW]	8040
MEP [bar]	21
Speed [rpm]	95

3. CFD simulation results

3.1. Design variables

The CFD model described in the previous section was utilised as a predictive tool to evaluate different design concepts of components that play a key role to the combustion process. The dual fuel combustion concept under consideration relies on the ignition of methanol after its interaction with the pilot flame. Since the injector nozzle tip (Figure 6) determines the distribution of fuel inside the cylinder and the interaction of the main fuel with pilot flame, its impact on combustion is crucial.

The use of methanol as the main fuel for combustion leads to a significant increase of injected fuel quantity, when compared to standard diesel, due to its lower calorific value. The required higher fuel flow can be managed through increasing the rail pressure, increasing the nozzle holes diameter, or prolonging injection duration. Such strategies impact spray penetration and in case of nozzle hole diameter increase, the spray atomization. In this study the design of the nozzle tip, and specifically, the number of holes, size and characteristic angles were varied to evaluate their effect with respect to spray formation, heat release, and pollutant formation.

Figure 6: baseline injector nozzle tip

Figure 7 depicts two different nozzle tips where the characteristic angles of each hole where changed, while preserving the overall flow area, and therefore the injection duration and mass flowrate. The heat release rates resulting from the two different nozzle tip configurations, which were compared under the same engine operating conditions, are shown in Figure 8.

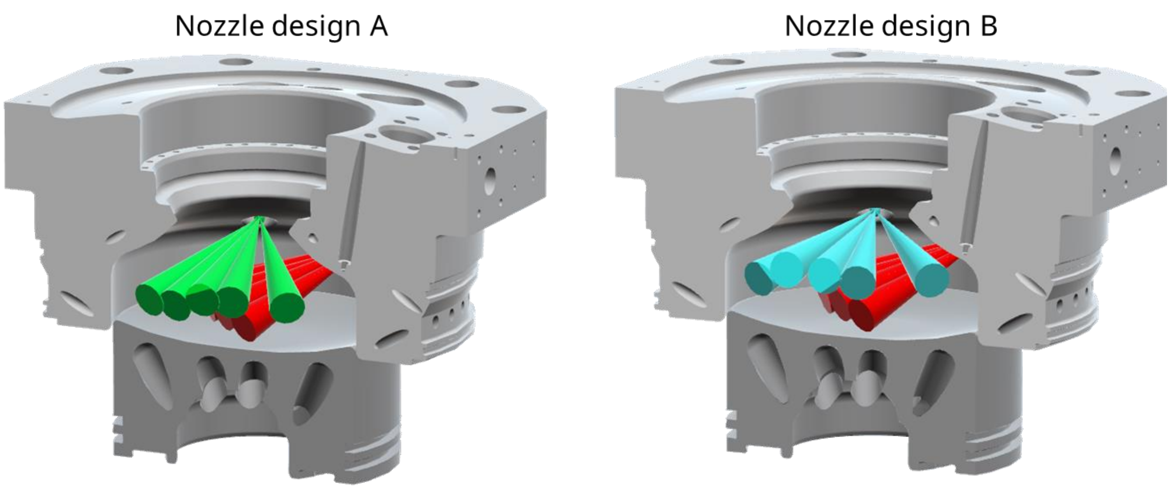

Figure 7: Comparison of methanol nozzle tip designs A and B

The heat release analysis shows a first energy spike, accounting for 5% of the total, due to the pilot fuel ignition, followed by the energy released from methanol combustion. Focusing on the methanol combustion from the two nozzle tips, it is evident that a different heat release evolution takes place between nozzle design "A" and "B". The analysis showed that nozzle "A" provided a non-optimal spray interaction between the pilot and main fuels, which led to an initial premixed combustion phase and an abrupt heat release, whereas nozzle "B" showed a smoother ignition of methanol that resulted to a more controllable in-cylinder pressure rise and heat release.

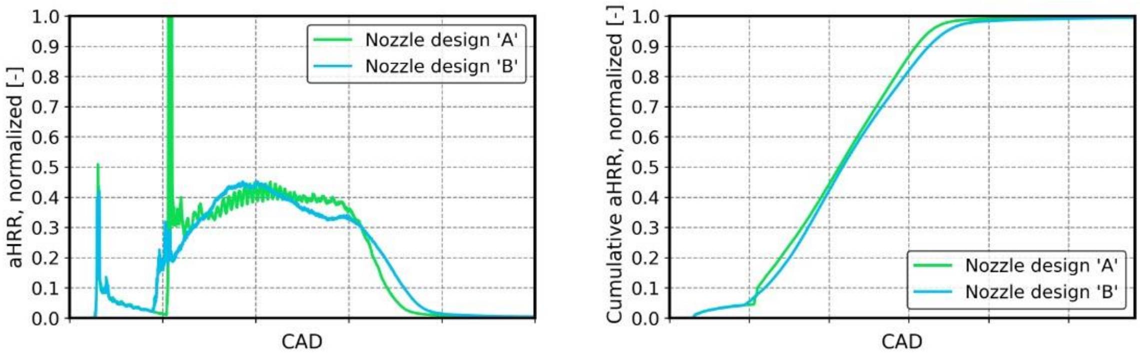

Figure 8: Nozzle tip design comparison (A vs B) with respect to heat release and cumulative heat release rate

The major impact from the nozzle tip design is clearly evident on the spray penetration and fuel mixing, as shown in figure 9 that compares nozzles "A" and "B". The blue colour contours represent the stochiometric iso-surfaces of methanol at same CAD. It can be seen that Nozzle "A" causes a narrow spray distribution, in relation to design "B", and creates a richer mixture plume in the earlier phases of combustion (5° after SOI). In the later stages of combustion, the more compact spray of Nozzle "A" had a strong impact on fuel penetration, with higher tendency to interact with the walls, increasing the risk of higher thermal stresses on components, and the formation of unburned hydrocarbons.

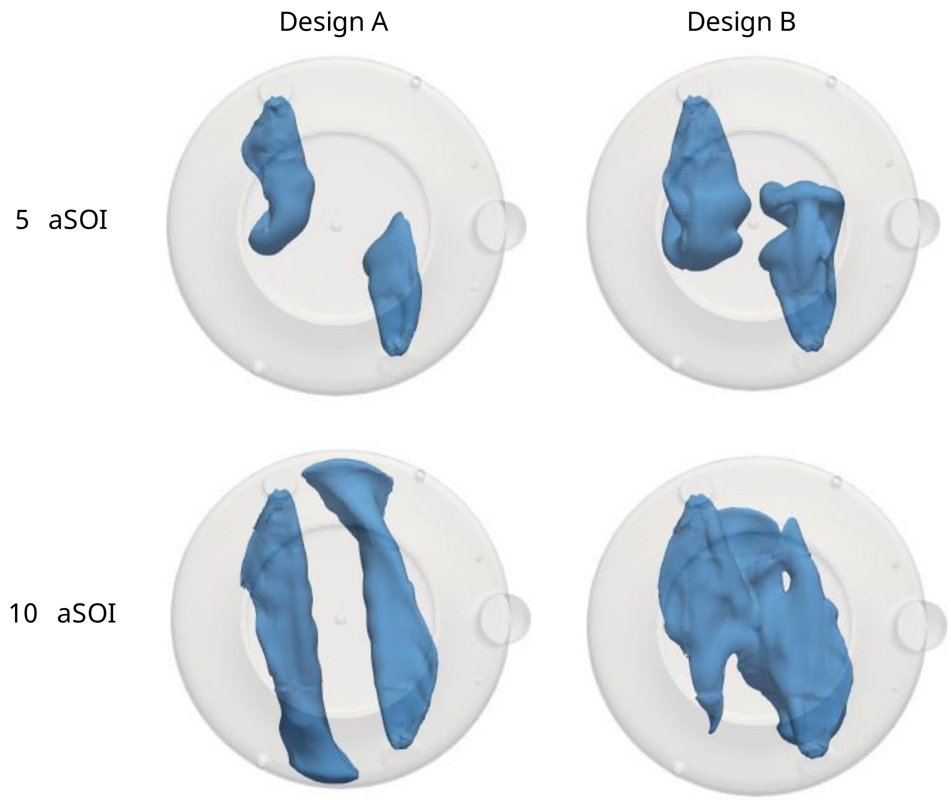

Figure 9: Comparison of Methanol stochiometric iso-contours from Nozzle tip designs A and B

The sensitivity analysis of the nozzle diameter involved scaling the dimension of each hole by ±30% with respect to the baseline design (Figure 10). The increase in flow area allowed for a shorter injection duration, and consequently faster combustion, but also led to higher combustion temperatures and longer spray penetrations. On the other hand, the reduction of the flow area was beneficial for spray penetration, but increased the combustion duration while decreasing the peak firing pressure and therefore deteriorating combustion efficiency.

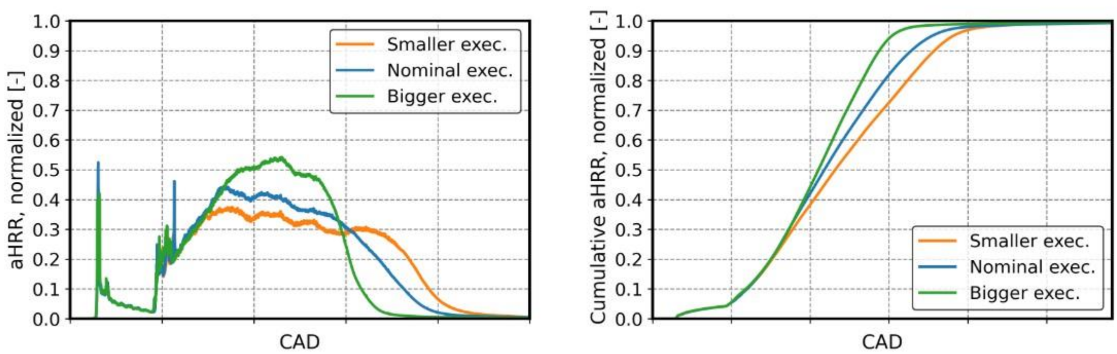

Figure 10: aHRR and cumulative aHRR trace effect on variation of nozzle hole diameters

A visualization of the in-cylinder flame development, represented by gas temperature iso-contour at 2300 K, is depicted in Figure 11. The results confirmed the different evolution of the flame between the two designs, showing that in the case of bigger hole diameters (Figure 11a) the spray penetrates further into the combustion chamber, leading to a strong flame/liner interaction, whereas with the smaller hole sizes a significantly shorter flame depth was observed with negligible flame-wall contact (Figure 11b).

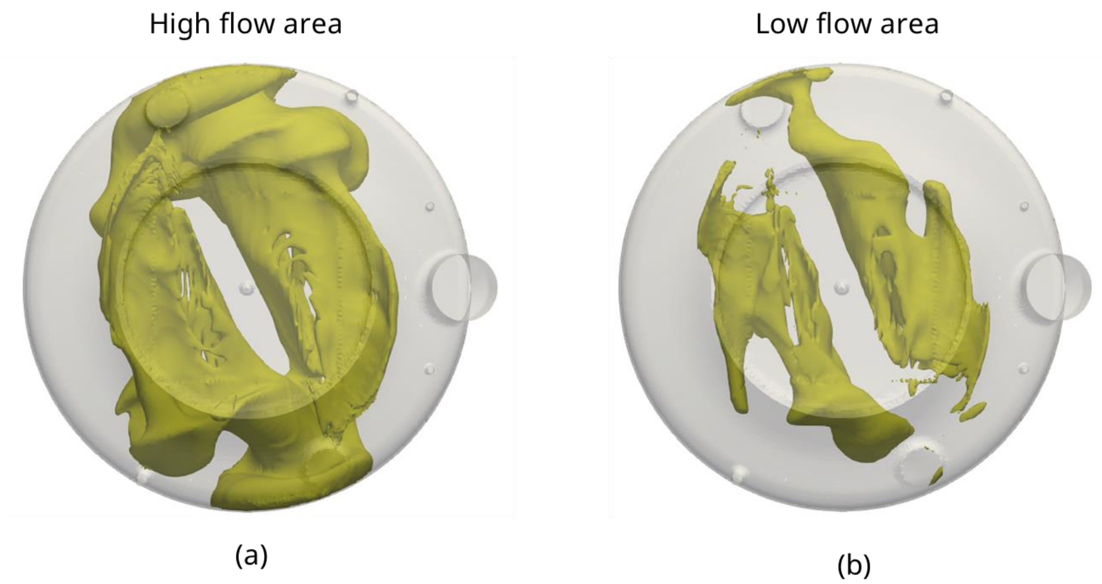

Figure 11: Flame temperature iso-contour visualization - (a): High flow area (1.3 x nominal Area) – (b) Low flow area (0.7 x Nominal)

Further investigation of the nozzle design characteristics involved a sensitivity analysis on the injection timing, and specifically the interval between the pilot fuel and main fuel injection events, hereafter referred as "dwell time". It was observed that dwell time, in combination to the nozzle tip geometry and engine load, had a strong impact on in-cylinder pressure. A sweep of the dwell time, with pilot SOI activated pre and post the main fuel SOI, and its effect on in-cylinder pressure is depicted in Figure 12. It can be seen that as the dwell time is reduced (i.e. shifted from after the main fuel SOI to before the main fuel SOI) an increase in firing pressure takes place. By starting the main fuel injection before the pilot fuel injection, methanol has sufficient time to vaporize and mix with air prior to the ignition of the pilot fuel. Consequently, when the pilot fuel ignites methanol initially burns in premixed combustion, followed by diffusive combustion as methanol injection continues to take place even after the pilot fuel injection terminates.

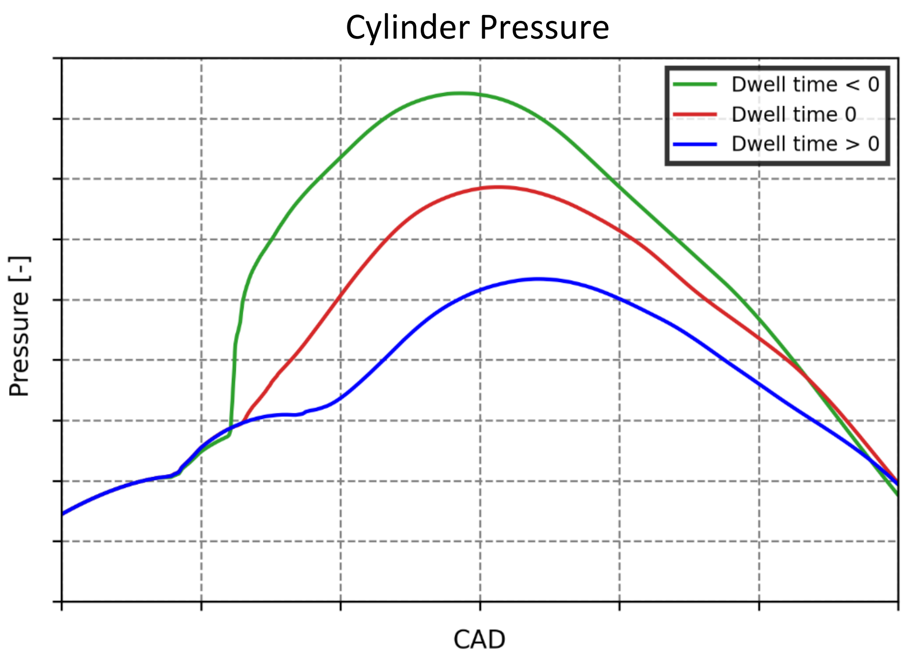

Figure 12: Effect of dwell time on in-cylinder pressure

All the above-mentioned parameters were considered for the selection of the Methanol and Diesel nozzle tip that were manufactured and subsequently tested on the RTX5 experimental engine.

4. Diesel engine conversion to Dual Fuel

To enable dual fuel operation, the engine was retrofitted with a methanol fuel injection system, while the original diesel fuel injection system was kept unchanged. As a result, in the event of failure of any of the methanol system components, the engine would switch automatically to Diesel mode operation, ensuring its continuous and safe operation.

4.1. Engine fuel components

The selected methanol fuel injection system consisted of a high-pressure reciprocating piston pump that was located inside the engine room, and a methanol dedicated fuel injection system that was located on the engine and consisted of a common rail that fed fuel to two injectors on each cylinder.

The high-pressure pump was equipped with flow control valves that ensured smooth operation throughout the full engine load range. Additionally, a drain valve was incorporated in the pump's skid to safely discharge methanol outside the engine room in case of an emergency.

The on-engine methanol fuel injection system was based on already existing Wärtsilä RT-Flex engine components, that were modified to accommodate methanol as the working fluid.

More specifically, the common rail was connected to high pressure pipes from the high-pressure pump and was large enough to account for the lower calorific value of methanol, compared to that of diesel, and ensured sufficient amount of fuel to the injectors and stable injection events. Six injection control units (ICUs), one for each cylinder, were installed on the methanol common rail, and through hydraulic -actuation these monitored and controlled the amount of fuel that was injected per cylinder. To address the low lubricity of methanol, the reciprocating components inside the injection control unit were coated with a solid lubricant. Additionally, multiple sealing barriers, both solid and fluid, were installed to prevent possible fuel leaks into the hydraulic actuation system.

The injectors were symmetrically positioned on the cylinder cover, at a specified distance from the diesel injectors. As with the ICUs, the moving components of the methanol injection valves were coated with a solid lubricant to compensate for methanol's low lubricity. Furthermore, pressure sensors were installed at the inlet port of each injection valve for injection event and combustion diagnosis purposes.

4.2. Engine safety components

The methanol fuel supply and injection systems incorporated also a number of safety features to ensure a safe and reliable operation of the engine. With methanol being a low flash-point fuel the fuel supply pipes and all pipes operating at high pressures were required to have secondary barriers in order to collect possible fuel leakages caused by misalignments between the mating surfaces of pipe connections or pipe leakages. Additionally, the methanol common rail was equipped with an encapsulation and an air ventilation system to contain and remove possible fuel leakage during the engine operation. A series of gas detectors were also installed within the encapsulated volume to ensure the methanol concentration in the spaces monitored remained as low as possible, and within the 20% of the Lower Explosive Limit (LEL), in accordance with Classification Societies requirements (Figure 13).

A hydraulically-actuated safety valve, controlled via the engine control system, allowed for depressurisation of the methanol fuel system in case of engine failure. Nitrogen and drain valves were used to purge methanol from the fuel injection system in the event of a major failure or other hazardous events in the engine room.

To facilitate maintenance works and overhauls, additional safety measures were adapted to ensure that the fuel system could be effectively and completely purged from methanol. For this purpose, a parallel connection in the low-pressure piping system, upstream of the high-pressure pump, enabled diesel oil to be supplied into the methanol fuel system. A pair of shut-off valves were used to stop the low-pressure methanol supply and to start the diesel supply into the high-pressure pump. Any methanol trapped inside the fuel injection system was then gradually consumed by the engine, leaving only diesel oil inside the fuel pipes and components, therefore enabling the safe removal and maintenance of all methanol related components (Figure 14).

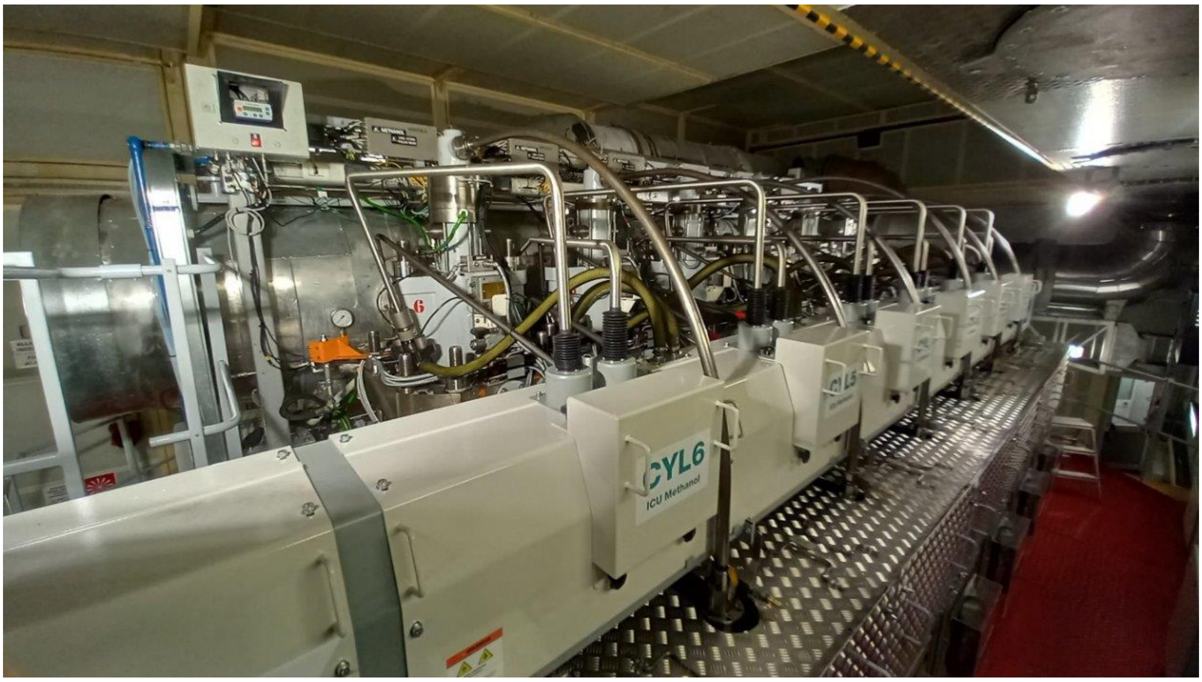

Figure 13: On-Engine methanol injection system: ventilated encapsulation of common rail and injection control units

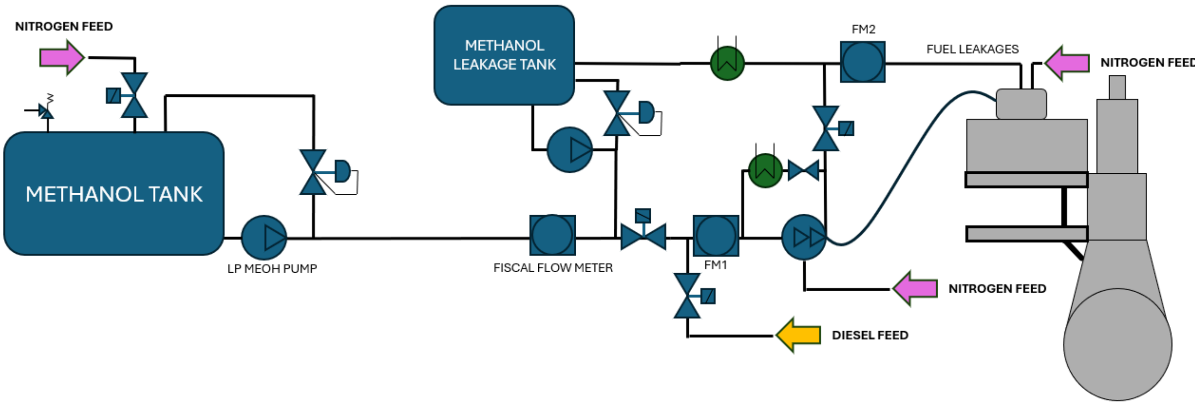

Figure 14: Schematic of the methanol fuel supply systems of 2-stroke R&D engine (RTX5)

5. Engine tests and Experimental results

RTX5 is an R&D engine that is used for investigation purposes of various technologies, prior to adaptation and implementation of these technologies on vessels. It is a fully instrumented engine with different types of sensors that can monitor and collect data about the performance of the engine and the condition of key components and systems. Measurements included the thermal load of components, pressures and temperatures in various locations such as the intake system, cylinder and exhaust system, and flows, such as fuel consumption. Furthermore, emission analysers were installed in the exhaust system of the engine that measured pollutants such as unburned hydrocarbons, CO, CO_2, NO_x, potential methanol slip and formaldehyde emissions.

The methanol combustion system, that was developed initially through CFD simulations, was further validated on RTX5 during the experimental campaign, where the engine was operated at different ratings on both, Methanol and Diesel modes. For clarity purposes the work described in this study corresponds to one of the various ratings tested, the 21 bar MEP, at a power of 8040 kW and 95 rpm, which is representative of typical 2-stroke marine diesel engines.

As a first step, tests were conducted on diesel mode at four engine loads (25%, 50%, 75% and 100%) to create a baseline for the performance of the engine, while the NO_x emissions of the engine were kept within the Tier II limits. Subsequently, the engine was run in methanol mode at the same firing pressure as that of the diesel mode operation so that the two fuel modes could be directly compared on combustion efficiency. The results from the two sets of tests, at 75% engine load are depicted in Figures 15 and 16. Figure 15 shows that the fuel consumption in Methanol operation, which also includes the pilot fuel consumption, was reduced by about 5% compared to that of diesel mode. Furthermore, at the same engine load, figure 16 shows that NO_x emissions during methanol operation were 40% lower than those measured during diesel operation. Both, the improved fuel consumption and lower NO_x emissions were attributed to the improved thermal efficiency and lower combustion temperatures achieved during methanol operation. Figure 17 compares the in-cylinder pressure and heat release rate of the two fuel modes at 75% engine load, based on in-cylinder pressure trace data that was recorded and averaged over 300 engine cycles. The results show that the methanol and diesel heat release rates are very similar, but also demonstrate the relatively faster combustion of methanol compared to diesel, that explains the above observations about the improved fuel consumption.

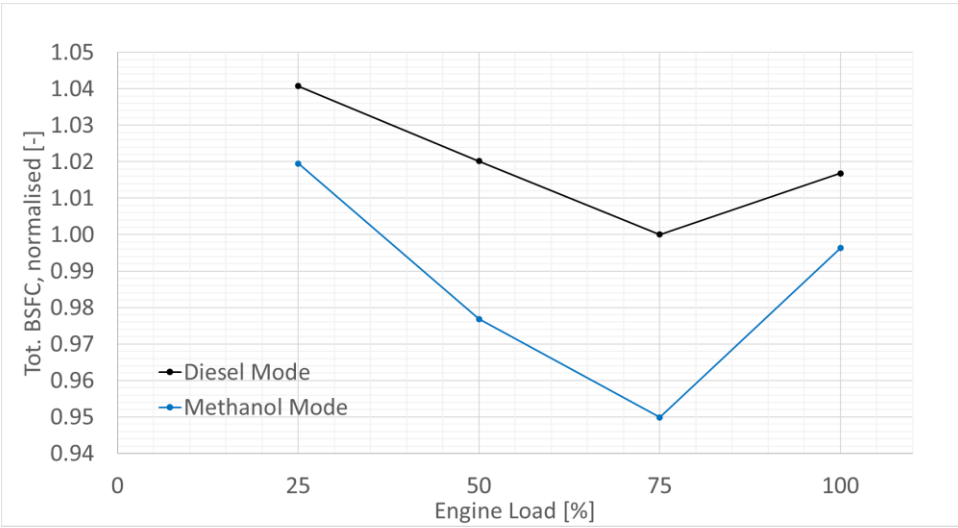

Figure 15: Brake-specific fuel consumption (BSFC) for operation on Methanol and Diesel Modes, at 75% engine load

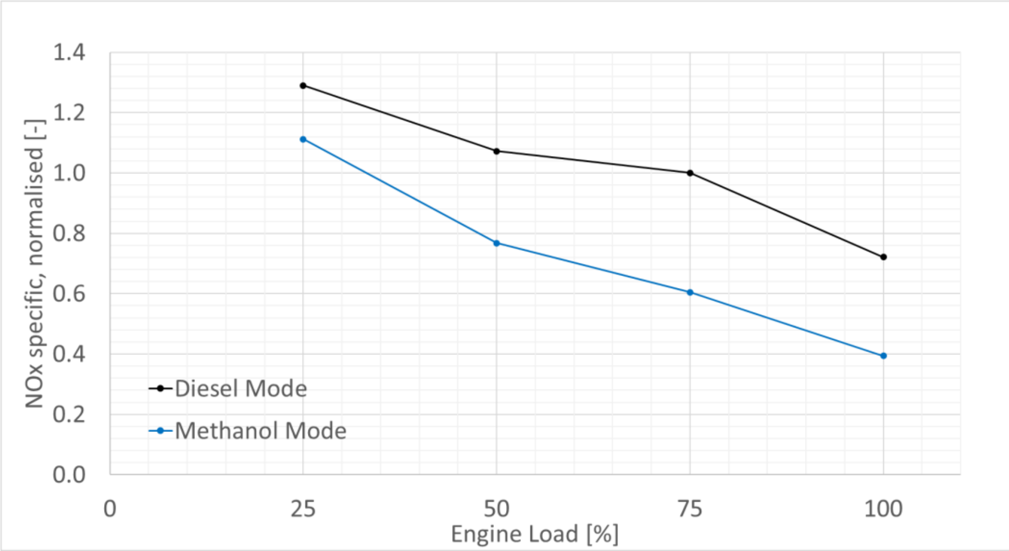

Figure 16: Specific NOx Emission on Diesel and Methanol modes, at 75% of engine load

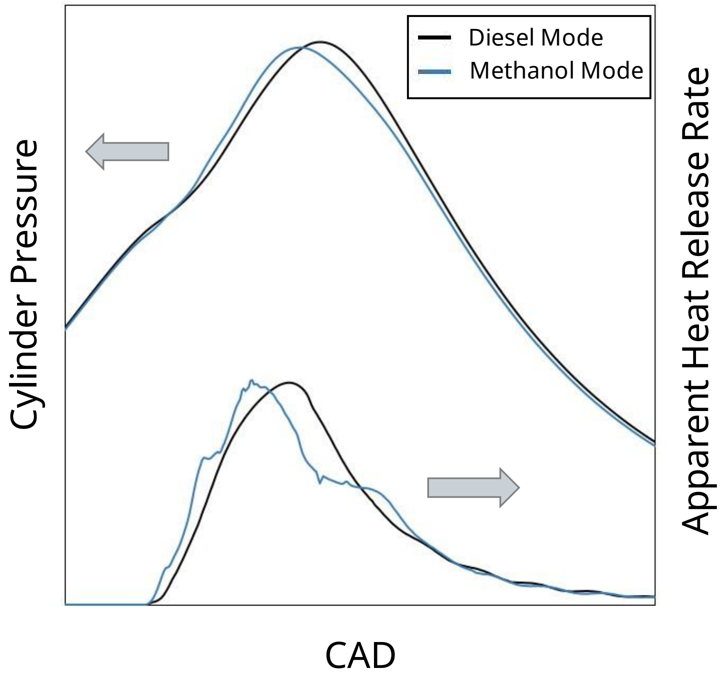

Figure 17: In-cylinder pressure and Heat release rate for operation on Methanol and Diesel modes, at 75% engine load (21bar MEP)

6. Engine Model Validation

The experimental tests on RTX5 engine provided a data base for the validation of the CFD simulations that were conducted prior to the tests to develop the methanol combustion system. The model validation was performed for selected cases of engine running, where a complete engine simulation was run to replicate the experimental boundaries.

For clarity, only two representative validation points are reported in Figure 18, where experimental data from operation in diesel and methanol modes are compared to the CFD simulation results. The plots show that the measured and simulated pressure curves and heat release are in good agreement for either fuel. Comparing the two fuel modes, both the experimental and simulated results capture the relatively longer combustion phase of diesel when compared to methanol, attributed to the faster burn of the latter.

Similar observations were made for all the other engine loads tested, the various engine tuning settings and the different nozzle tip designs that were evaluated on the engine. The good correlation between the experimental data and simulations demonstrated that the adopted CFD methodology can be successfully used as a predictive tool for the development of combustion systems of different fuels and the definition of nozzle tip designs, which can be applied as retrofit technology to existing 2-stroke marine diesel engines, and enable these to be converted to dual-fuel engines.

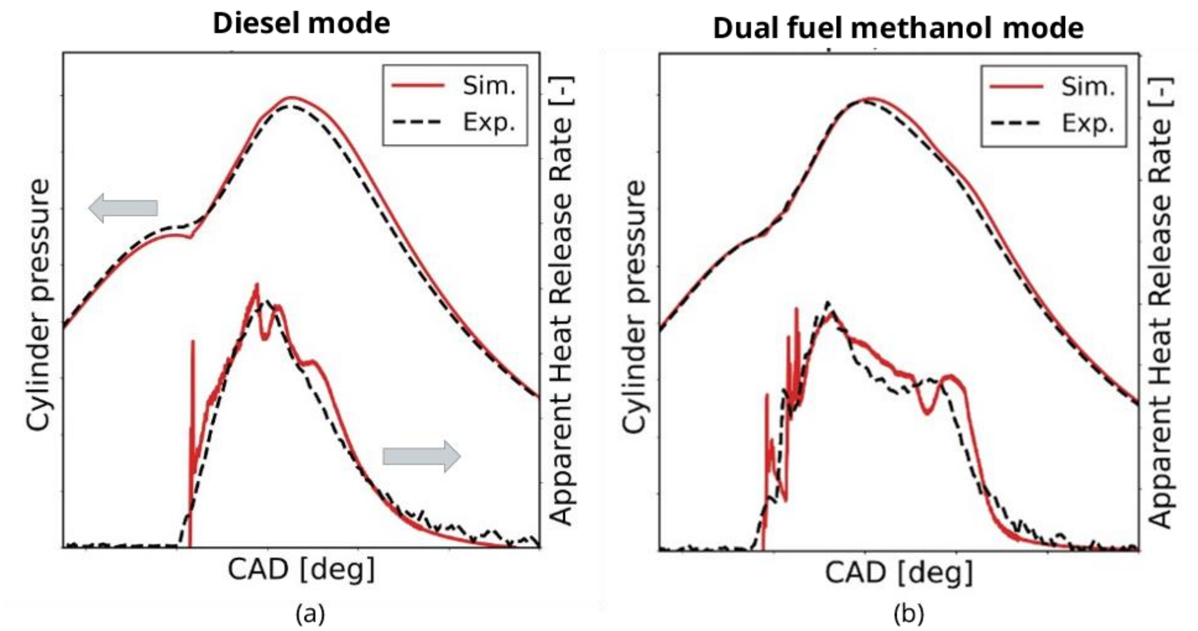

Figure 18: Comparison between Experimental data and CFD: In-cylinder pressure and Heat release rate for operation on (a) Diesel and (b) Methanol modes, at 75% engine load (21bar MEP)

7. Conclusions

This study described the different stages that were followed to conceptualise, design and develop a robust dual-fuel combustion system, which will be implemented to an innovative retrofit kit and enable existing marine diesel engine to be converted to dual-fuel engines and operate on sustainable fuels. The physical properties of methanol, such as its lower calorific value, its low lubricity and corrosive nature, were all considered in the design and sizing of the systems and components. The dual-fuel combustion concept was first analysed thoroughly by CFD simulations, focusing on the main parameters that characterize methanol combustion. The analysis was also used to design an important component for the combustion system, the injector nozzle tip. The analysis was followed by tests on an experimental engine, where the combustion system was validated and further developed. The results from the testing campaign demonstrated excellent engine running stability at different loads and speeds with a minimum quantity of pilot fuel injected. At the end of the test campaign and after analysing the engine performance and emission results it was shown that the fuel consumption in methanol can be lower than that of diesel mode, as well as the NO_x emissions that were reduced significantly. The performance improvement and emission reductions can be explained by the lower combustion temperatures and the improvement on the thermodynamic efficiency achieved on methanol operation.

The study concluded that methanol as a main fuel for 2-stroke marine engines is a viable and promising solution in the decarbonisation of shipping.

Abbreviations

aHRR – Apparent heat release rate

aSOI – After start of Injection

BSFC – Brake specific fuel consumption

CAD – Crank angle degree

CFD – Computational fluid dynamics

CNR STEMS – Consiglio Nazionale delle Ricerche, Istituto di scienze e tecnologie per l'energia e la mobilità sostenibili

CO - Carbon monoxyde emission

DI - Direct injection

GHG – Green House Gas

HC – Unburned hydrocarbon emission

ICU – injection control units

MEP – Mean effective pressure

NO_x – Nitrogen oxides emission (NO, NO2)

PFI – Port fuel injection

RANS – Raynolds averaged Navier-Stokes equation

RON - Research Octane Number

RTX5 – Wärtsilä 6RT-Flex50-B – Test engine for R&D activities

Literature

[1] Verhelst, S., Turner, J., Sileghem, L., and Vancoillie, J.(2019) Methanol as a fuel for internal combustion engines, Progress in Energy and Combustion Science, Vol. 70, 2019, Pages 43-88, ISSN 0360-1285, https://doi.org/10.1016/j.pecs.2018.10.001.

[2] Cheng C., Faurskov Cordtz R., Dyhr Pedersen T., Winther K., Langballe Førby, N. & Schramm, J. (2023). Investigation of Combustion Characteristics, Physical and Chemical Ignition Delay of

Methanol Fuel in a Heavyduty Turbo-charged Compression Ignition Engine. Fuel, 348, Article 128536. https://doi.org/10.1016/j.fuel.2023.128536

[3] Nylund, N.-O., Murtonen, T., Westerholm, M., Söderström, C., Huhtisaari, T., & Singh, G. (2015). *Testing of various fuel and additive options in a compression-ignited heavy-duty alcohol engine*. ISAF-0056. Paper presented at 21st International Symposium on Alcohol Fuels, ISAF, Gwangju, Republic of Korea.

[4] Shamun S., Haşimoğlu C., Murcak A., Andersson ö , Tunér M., Tunestål P. (2017) Experimental investigation of methanol compression ignition in a high compression ratio HD engine using a Box-Behnken design, Fuel,Volume 209,2017, Pages 624-633, ISSN 0016-2361, https://doi.org/10.1016/j.fuel.2017.08.039.

[5] Jia Z., Denbratt I., (2018) Experimental investigation into the combustion characteristics of a methanol-Diesel heavy duty engine operated in RCCI mode, Fuel, Volume 226, 2018, ages 745-753, ISSN 0016-2361, https://doi.org/10.1016/j.fuel.2018.03.088.

[6] Repo J., Axelsson M., Heir V. (2023) Methanol combustion concept alternatives for new build and retrofit of 4-stroke medium speed engines, Paper presented at 30th CIMAC Congress 23, Busan, Korea

[7] Dong Y., Kaario O., Hassan G., Ranta O., Larmi M., Johansson B. (2020) High-pressure direct injection of methanol and pilot diesel: A non-premixed dual-fuel engine concept, Fuel, Volume 277,2020,117932, ISSN 0016 -2361, https://doi.org/10.1016/j.fuel.2020.117932.

[8] Coppo M., Negri C., Wermuth N., Garcia-Oliver J. M., Cao J. (2023) Powering a greener future: the OMT injector enables high-pressure injection of ammonia and methanol, Paper presented at 30th CIMAC Congress 23, Busan, Korea

[9] Sarathy S., Oßwald P., Hansen N., Kohse-Höinghaus K., (2014) Alcohol combustion chemistry, Progress in Energy and Combustion Science, Volume 44, 2014, Pages 40-102, ISSN 0360-1285, https://doi.org/10.1016/j.pecs.2014.04.003.

[10] Lucchini T., Della Torre A., D'Errico G., Onorati A. (2019) Modeling advanced combustion modes in compression ignition engines with tabulated kinetics, Applied Energy, Volume 247, 2019, Pages 537-548, ISSN 0306-2619, https://doi.org/10.1016/j.apenergy.2019.04.062.

[11] Sementa P., Lazzaro M., Tornatore C., Catapano F., Calvo Oliveira A., Thorsen L., Viglione L. (2024) Experimental Investigation of High-Pressure Ammonia Spray and Combustion under Marine Engine-Like Conditions Using Optical Diagnostics, THIESEL 2024 Conference on Thermo- and Fluid Dynamics of Clean Propulsion Powerplants

[12] Schirru, A., Hardy, G., Wright, Y.M., Lucchini, T. et al. (2023), "CFD Modeling of a DME CI Engine in Late-PCCI Operating Conditions," SAE Technical Paper 2023-01-0203, 2023, doi:10.4271/2023-01-0203

[13] Zhang K., Banyon C., Bugler J., Curran H. J., Rodriguez A, Herbinet O., Battin-Leclerc F., B'Chir C., Heufer K. A. (2016) An updated experimental and kinetic modeling study of n-heptane oxidation, Combustion and Flame, Volume 172, 2016, Pages 116-135, ISSN 0010-2180, https://doi.org/10.1016/j.combustflame.2016.06.028

[14] Pelucchi, M., Cavallotti, Faravelli, T., Klippenstein, S.J. (2018) H-Abstraction reactions by OH, HO2, O, O2 and benzyl radical addition to O2 and their implications for kinetic modelling of toluene oxidation, Physical Chemistry Chemical Physics, 20, pp. 10607-10627 (2018), DOI: 10.1039/C7CP07779C

[15] Tekgül B., Peltonen P., Kahila H., Kaario O., Vuorinen V. (2021) DLBFoam: An open-source dynamic load balancing model for fast reacting flow simulations in OpenFOAM, Computer Physics Communications, Volume 267, 10.1016/j.cpc.2021.108073 (2021).